J Nanostruct 13(1): 48-58, Winter 2023

RESEARCH PAPER

How Is Photocatalytic Activity of $TiO_2/In_2S_3/Cu$ and $TiO_2/In_2S_3/Ag$ Nanocomposites under Visible Light?

Sangar S. Ahmed

Chemistry Department, College of Science, Salahaddin University, Kirkuk Road, Erbil, Kurdistan Region, Iraq

ARTICLE INFO

Article History:
Received 16 September 2022
Accepted 18 December 2022
Published 01 January 2023

Keywords:
Nanostructures
Organic Pollution
Photocatalyst
$TiO_2/In_2S_3/Ag$
$TiO_2/In_2S_3/Cu$

ABSTRACT

In present work $TiO_2/In_2S_3/Cu$ and $TiO_2/In_2S_3/Ag$ nanocomposites were prepared as a highly efficient photocatalyst. In this design, $TiO_2/In_2S_3/Ag$ and $TiO_2/In_2S_3/Cu$ composites enjoy both co-sensitizer and plasmonic effects. $TiO_2/In_2S_3/Cu$ nanocomposites and $TiO_2/In_2S_3/Ag$ nanocomposites were applied to purify wastewater containing Rhodamine B, Methyl orange, Acid Black 1, and Acid Brown 214. $TiO_2/In_2S_3/Cu$ nanocomposites and $TiO_2/In_2S_3/Ag$ nanocomposites show significant improvement in degradation efficiency compared to the bare TiO_2. As-prepared $TiO_2/In_2S_3/Cu$ and $TiO_2/In_2S_3/Ag$ nanocomposites were characterized by different methods such as XRD, EDX, and SEM.

How to cite this article
Ahmed S S. How Is Photocatalytic Activity of $TiO_2/In_2S_3/Cu$ and $TiO_2/In_2S_3/Ag$ Nanocomposites under Visible Light? J Nanostruct, 2023; 13(1):48-58. DOI: 10.22052/JNS.2023.01.006

INTRODUCTION

Recently, using photocatalysts for purifying water and wastewater has received incredible attention around the world because it works by a renewable source of energy. In addition, it operates at room temperature without additional power sources [1]. There are many different photocatalytic materials but TiO_2 is recognized as the excellent photocatalytic material due to its high oxidation potential, brilliant photoactivity, nontoxicity, physical and chemical stability, and earth abundancy [2-4]. It was illustrated that contaminant removal started by redox reactions on the surface of the catalyst. First, photon absorbed by the surface of catalyst and generates electron-hole pairs. These generated charge carriers migrate to the surface of the catalyst and contribute to a degradation reaction [5-7]. The produced holes generate hydroxyl radical by reacting with the surface-trapped H_2O. Hydroxyl radical could oxidize most organic/inorganic pollutants [8]. On the other hand, the photogenerated electrons react with O_2 and produced $O_2^{\cdot-}$ radicals [8].

Various synthesis methods have developed to increase the surface area of the catalyst, for example, producing TiO_2-based nanoparticles, [9, 10] and nanorods, [11, 12]. An important issue that should be solved is that electron-hole pairs in TiO_2 just generated by absorption the ultraviolet (UV) range (~5 % of the solar spectrum). This happens due to the large band gap of TiO_2 (> 3.0 eV for rutile). In this case, much of the sunlight cannot be

* *Corresponding Author Email: sangar.ahmad1@su.edu.krd*

used for a photocatalytic reaction [13, 14].

Many types researches were done to solve this problem by decreasing the band gap by doping pure TiO_2 with a dopant such as N, Fe, S, etc. [15, 16]. The additional energy states generated by adding dopant can extend the absorption spectrum of TiO_2 to the visible range but intermediate energy states from the introduced atoms and defects can serve as traps and increases electron-hole recombination rate. This could drop off the degradation efficiency for doped TiO_2 [17-19]. Therefore, decreasing the band gap of TiO_2 by adding dopant is not a suitable solution. Physically or chemically attaching a heterogeneous material (called a co-sensitizer) on TiO_2 could be a brilliant solution. This can extend the absorption peak of TiO_2 to visible range in the in an efficient and more flexible way. Typical photocatalytic materials such as CdS and CdSe have been used as a sensitizer to change the band gap and extend the absorption peak of TiO_2 to the visible range [20, 21]. The Photogenerated electrons in sensitizer could transfer to the conduction band of TiO_2 If the conduction band of sensitizer located above the conduction band of TiO_2 [22-25]. However, choosing co- sensitizers are limited in terms of their water-solubility, toxicity, and performance.

In present work, we prepared $TiO_2/In_2S_3/Ag$ and $TiO_2/In_2S_3/Cu$ nanocomposite to achieve high photocatalytic activity under visible light. $TiO_2/In_2S_3/Ag$ and $TiO_2/In_2S_3/Cu$ nanocomposite enjoy both co-sensitizer and plasmonic effects. $TiO_2/In_2S_3/Ag$ and $TiO_2/In_2S_3/Cu$ nanocomposites were prepared by photo reduction and hydrothermal method. We studied the effect of different parameters such as reaction time and temperature on the morphology of $TiO_2/In_2S_3/Ag$ and $TiO_2/In_2S_3/Cu$ nanocomposites. As-prepared $TiO_2/In_2S_3/Ag$ and $TiO_2/In_2S_3/Cu$ nanocomposites show promising photocatalytic activity under visible light.

MATERIALS AND METHODS

Preparation of TiO_2/In_2S_3 composite

Firstly, 0.55 g of $InCl_3.4H_2O$ and 0.22 g of thioacetamide were dissolved into 40 mL of distilled water, and then TiO_2 was added into the solution. The mixture was transferred into stainless steel autoclave and heated at 140 C for 8 h. The samples were collected after being filtered and washed with distilled water and finally dried at 60 ◦C in air.

Preparation of $TiO_2/In_2S_3/Ag$ composite

Firstly, 0.25 g of $AgNO_3$ was dissolved into 40 mL of distilled water, and then TiO_2/In_2S_3 was added into the solution. The mixture was irradiated for 2 h under visible light. The samples were collected after being filtered and washed with distilled water and finally dried at 60 ◦C.

Preparation of $TiO_2/In_2S_3/Cu$

Firstly, 0.15 g of $Cu(NO_3)_2$ was dissolved into 40 mL of distilled water, then TiO_2/In_2S_3 composite was added into the solution. The mixture was irradiated for 2 h under visible light. The samples were collected after being filtered and washed with distilled water and finally dried at 60 ◦C.

Photocatalytic activity test

Certain amount of catalyst was dispersed in 50 mL water containing different organic pollution with 5 ppm in concentration. This suspension kept in dark place for 2 h to equilibrium dye absorption on the surface of the catalyst. Afterward, photocatalysis test was started by irradiation visible light with 400 W in power.

RESULTS AND DISCUSSION

In this research, we prepared $TiO_2/In_2S_3/Ag$ and $TiO_2/In_2S_3/Cu$ composites as efficient visible driven photocatalysts. $TiO_2/In_2S_3/Ag$ and $TiO_2/In_2S_3/Cu$ composites enjoy both co-sensitizer and plasmonic effects. The XRD patterns for TiO_2/In_2S_3, $TiO_2/In_2S_3/Ag$, and $TiO_2/In_2S_3/Cu$ composites are presented in Fig. 1 a-c, respectively. As can be seen in Fig. 1 a, TiO_2 has anatase phase and shows good agreement with JCPDS No. 21-1272. The XRD pattern of In_2S_3 could be assigned to β-In_2S_3 structure (JCPDS No. 65-0459). There are no impurities such as In_2O_3, InS or $In(OH)_3$, are detected. Fig. 1 b shows that $TiO_2/In_2S_3/Ag$ nanocomposite successfully prepared. We indicated peaks related to the Ag in Fig. 1 b. XRD pattern related to the $TiO_2/In_2S_3/Cu$ composites is illustrated in Fig. 1 c. Bedside the peaks related to the TiO_2/In_2S_3, peaks related to the Cu appeared. Fig. 2 a-c shows the EDX results for TiO_2/In_2S_3 nanocomposite, $TiO_2/In_2S_3/Ag$ nanocomposite, and $TiO_2/In_2S_3/Cu$ composites, respectively. Fig. 2 a shows the presence of Ti,

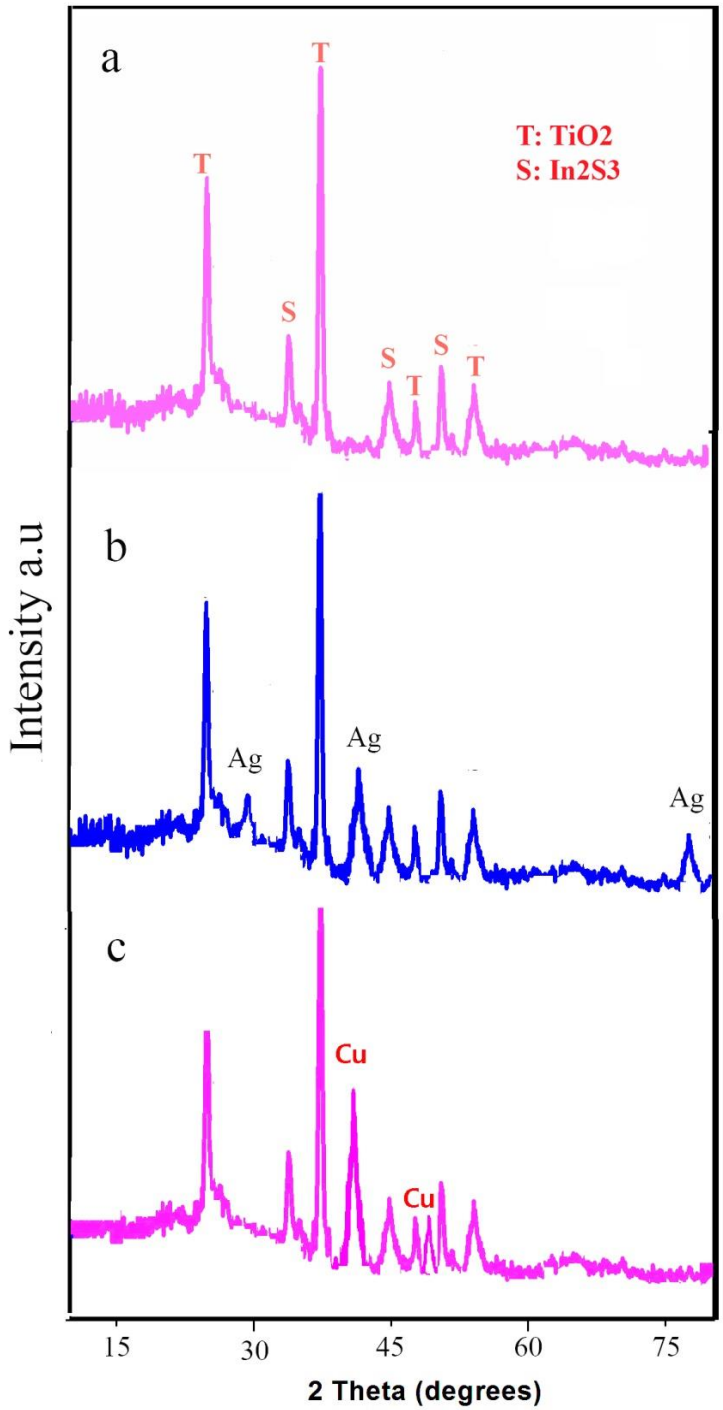

Fig. 1. XRD pattern of a) TiO_2/In_2S_3, b) $TiO_2/In_2S_3/Cu$ composite, and c) $TiO_2/In_2S_3/Ag$ nanocomposite.

O, In, and S elements related to the TiO_2/In_2S_3 nanocomposite. EDX presented in Fig. 2 b indicted that sample containing Ti, O, In, S, and Ag which could be assigned to $TiO_2/In_2S_3/Ag$ nanocomposite. According to Fig. 2 c, the sample is containing Ti, O, In, S, and Cu which are in good agreement with

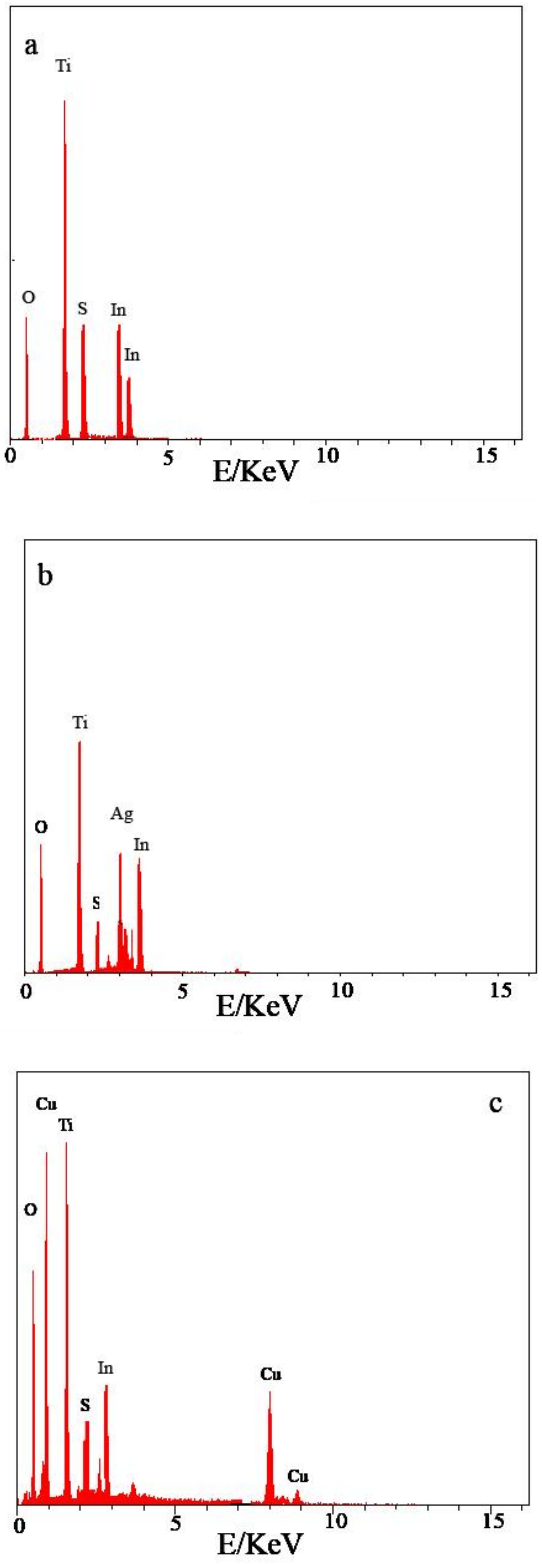

Fig. 2. EDX results for a) TiO_2/In_2S_3, b) TiO_2/In_2S_3/Cu composite, and c) TiO_2/In_2S_3/Ag nanocomposite.

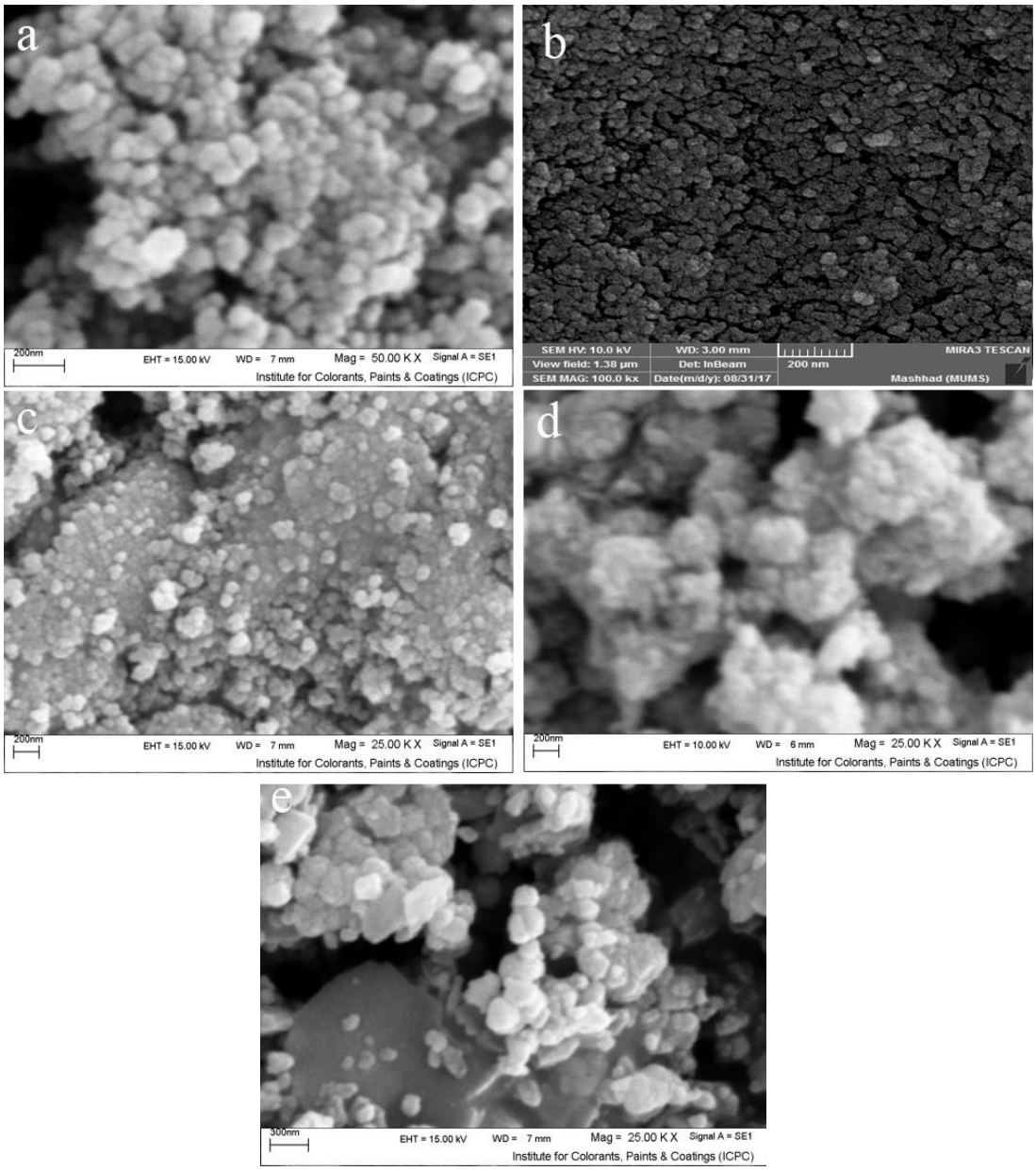

Fig. 3. SEM images of prepared $TiO_2/In_2S_3/Ag$ nanocomposite prepared a) 6h, b) 8h, c) 10, d)120 C, and e)160 °C.

$TiO_2/In_2S_3/Cu$ nanocomposite. Fig. 3 a- e shows the effect of hydrothermal time and temperature on the morphology of $TiO_2/In_2S_3/Ag$ nanocomposite. As seen in Fig. 3 a, $TiO_2/In_2S_3/Ag$ nanocomposite with an average size of 40- 150 nm were prepared when the reaction time and temperature were 6h and 140 °C. By changing the reaction time to 8h, very uniform $TiO_2/In_2S_3/Ag$ nanocomposite with 20- 40 nm in diameters were formed (Fig. 3 b). According to Fig. 3 c, particles with an average size of 40- 60 nm were formed when the reaction time was 10 h. Fig. 3 d shows that particles size are about 10-20 nm when the temperature was 120 °C. Particles size increased up to 1µm when reaction temperature was 160 C (Fig. 3 e). We studied the effect of reaction time on the morphology of $TiO_2/In_2S_3/Cu$ nanocomposite as well as. For these three different times including 6, 8, and 10 h was studied. Fig. 4 a shows $TiO_2/In_2S_3/Cu$ nanocomposites with 50-100 nm in

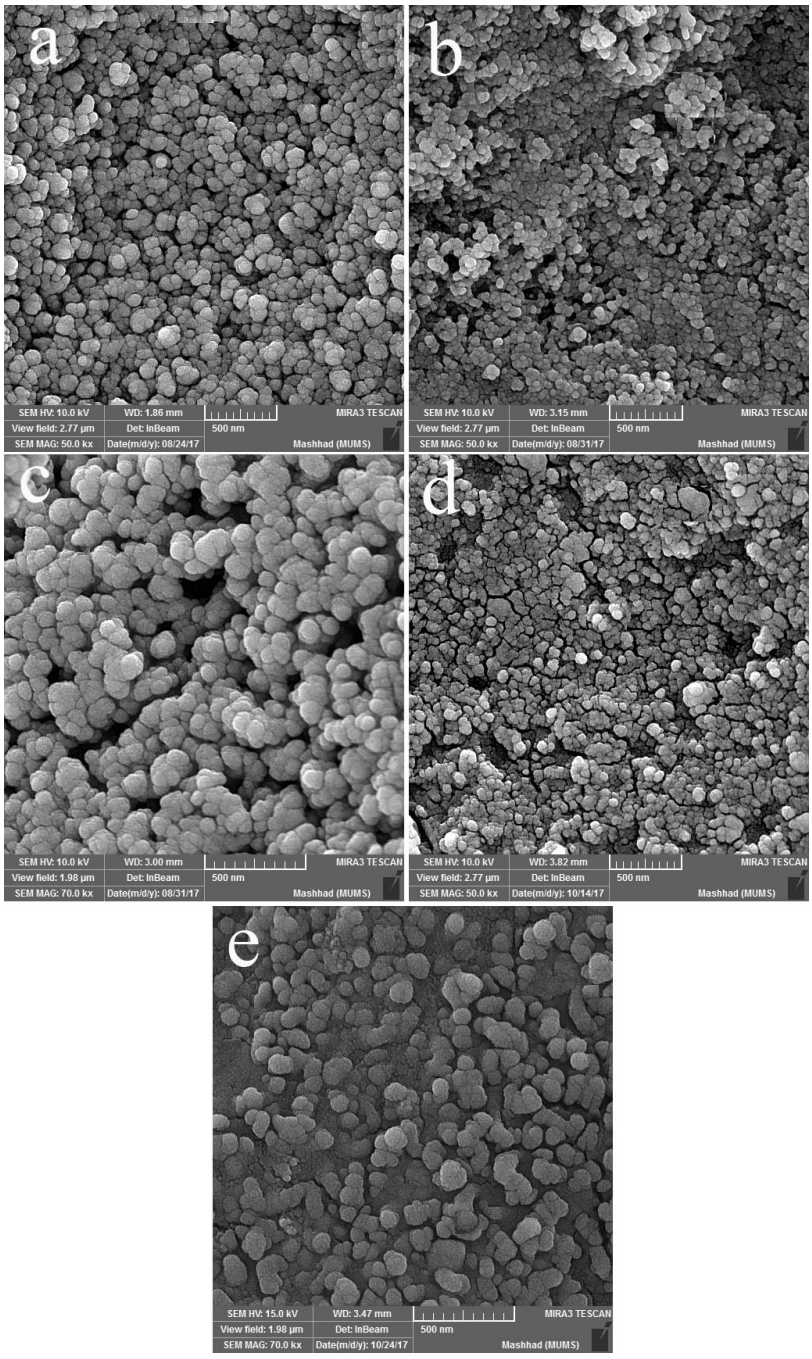

Fig. 4. SEM images of prepared $TiO_2/In_2S_3/Cu$ composite prepared a) 6h, b) 8h, c)10, d)120 C, and e)160 °C.

diameters were formed when the reaction time was 6 h. When reaction time was 8 h, Particles with size about 20- 50 nm were fabricated (Fig. 4 b). By changing the reaction time to 10 h, particles size increased to 50-150 nm (Fig. 4 c). The effect of reaction temperature on the morphology of $TiO_2/In_2S_3/Cu$ nanocomposites was evaluated by preparing $TiO_2/In_2S_3/Cu$ nanocomposites at 120,

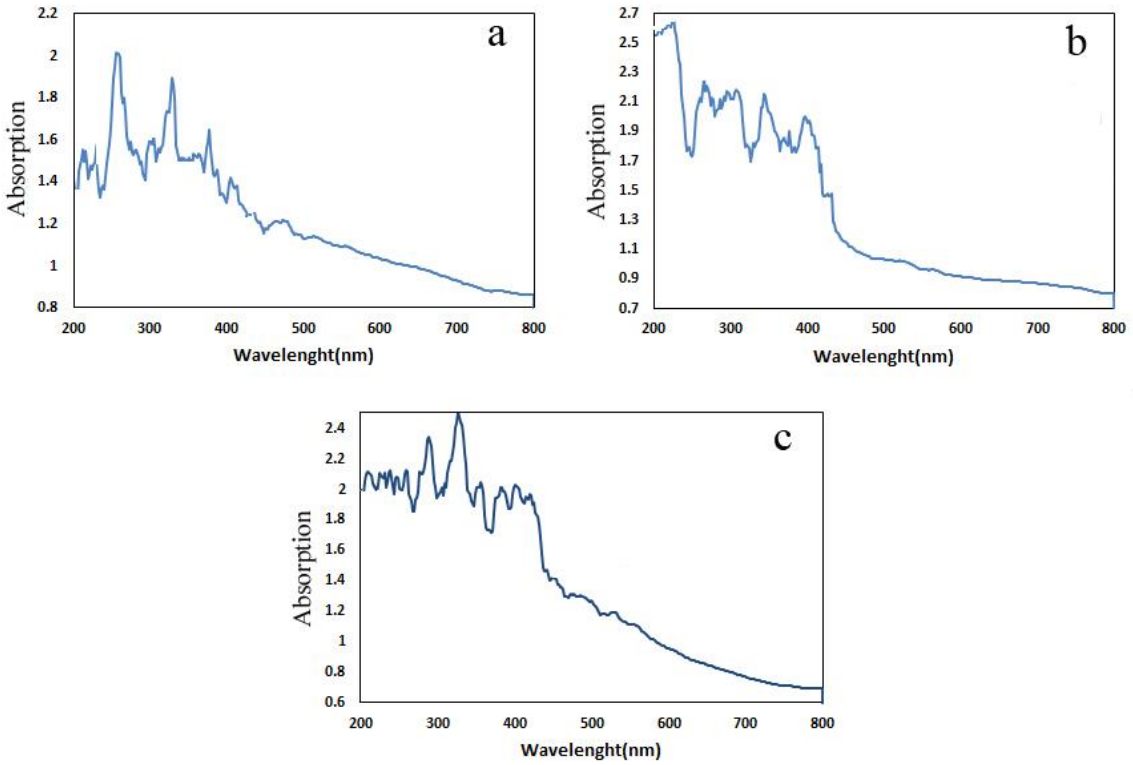

Fig. 5. DRS spectra of a) TiO_2/In_2S_3, b) TiO_2/In_2S_3/Ag composite, and c) TiO_2/In_2S_3/Cu nanocomposite.

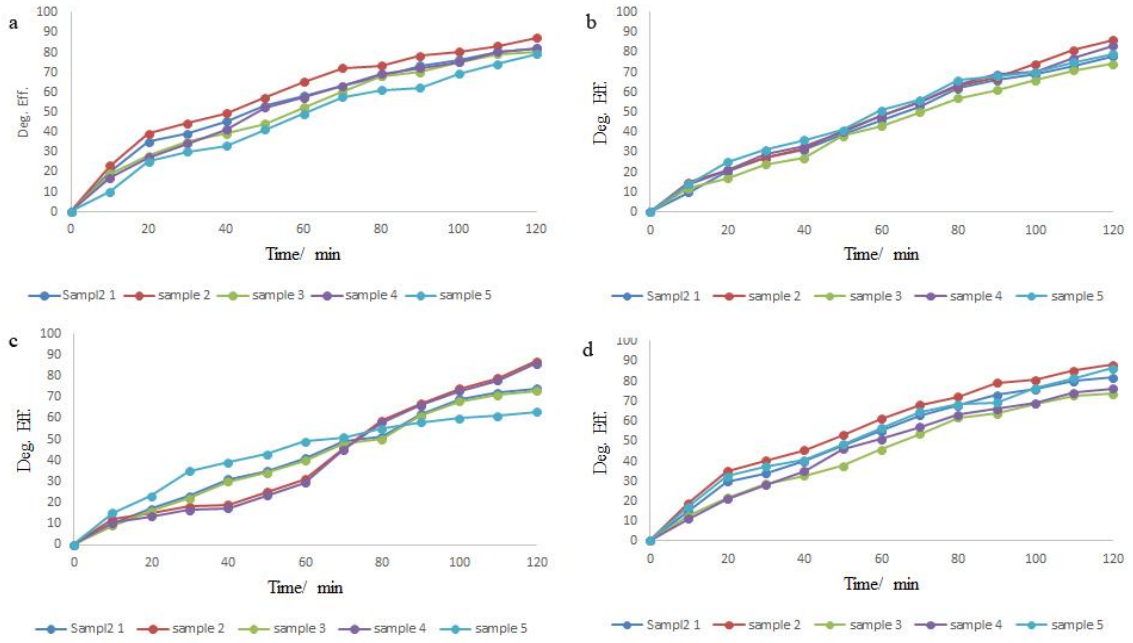

Fig. 6. Photocatalytic results of TiO_2/In_2S_3/Cu nanocomposite for a) RhB, b) MO, c) AB1, and AB214 under visible light for 120 min.

140, and 160 C. As can be seen in Fig. 4 d, large size distribution was observed when the reaction temperature was 120 °C (Fig. 4 d). By increasing the reaction temperature to the 140 C, more uniform particles are observed (Fig. 4 b). Particles stack together and form larger particles (about 200 nm) when reaction temperature was 160 C (Fig. 4 e).

We used Diffuse Reflectance Spectroscopy (DRS) to study the effect of In_2S_3, Ag, and Cu on the absorption of TiO_2. According to Fig. 5 a, TiO_2/In_2S_3 has the broad absorption peak from 200- 600 nm. As can be seen in Fig. 5 b and c, the absorption intensity of TiO_2/In_2S_3 was increased by adding Ag and Cu. It seems Ag had more significant effect due to the higher plasmonic effect [26, 27]. Based on these results, we can expect that $TiO_2/In_2S_3/Ag$ nanocomposites and $TiO_2/In_2S_3/Cu$ nanocomposites show highly photocatalytic activity under visible light.

We used Rhodamine B (RhB), Methyl orange (MO), Acid Black 1 (AB1), and Acid Brown 214 (AB214) as organic contaminations to study the photocatalytic activity of $TiO_2/In_2S_3/Cu$ nanocomposites and $TiO_2/In_2S_3/Ag$ nanocomposites. In all photocatalytic tests, the concentration of pollution was 5 ppm and 1 g/ L was catalyst was used. The results for the degradation of these four dyes by $TiO_2/In_2S_3/Cu$ nanocomposites under visible light for 120 min are presented in Fig. 6. As can be seen in Fig. 6 a, degradation efficiency for RhB was 82, 87, 80, 82, and 79 % for sample 1-5, respectively. The degradation efficiency was 78, 86, 74, 83, and 79 % for wastewater containing Mo (Fig. 6 b). When the organic pollutant was AB1, the degradation yield changes to 74, 87, 73, 86, and 63 % for sample 1-5, respectively (Fig. 6 c). Finally, the degradation rate of 81, 89, 73, 76, and 86 % were achieved when AB214 was used as an organic contaminant (Fig. 6 d).

When $TiO_2/In_2S_3/Ag$ nanocomposites were used as photocatalysts, the degradation efficiency was 85, 87, 80, 82, and 79 % for RhB (Fig. 7 a). As can be seen in Fig. 7 b, the degradation yield changes to 78, 84, 74, 82, and 78 % for sample 1-5 when the organic pollutant was MO. The degradation efficiency was 74, 84, 72, 78, and 76 % for wastewater containing AB1 (Fig. 7 c). By applying $TiO_2/In_2S_3/Ag$ nanocomposites to purify water containing AB214, 80, 87, 74, 78, and 85 % of AB214 was degraded in 120 min (Fig. 7 d).

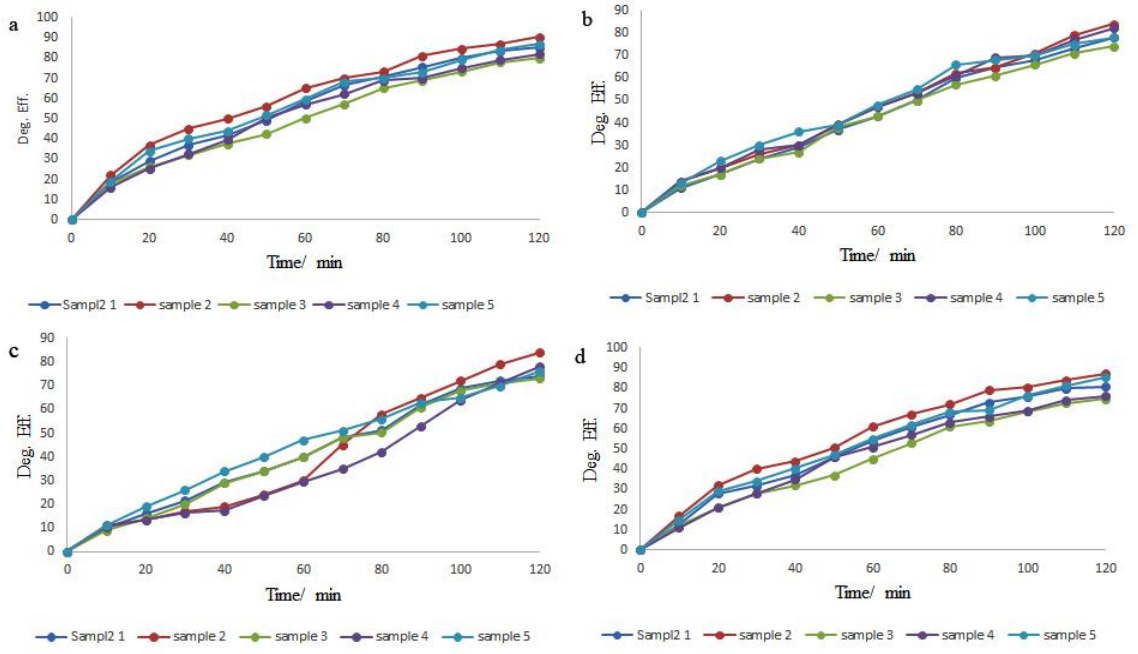

Fig. 7. Photocatalytic results of $TiO_2/In_2S_3/Ag$ nanocomposite for a) RhB, b) MO, c) AB1, and AB214 under visible light for 120 min.

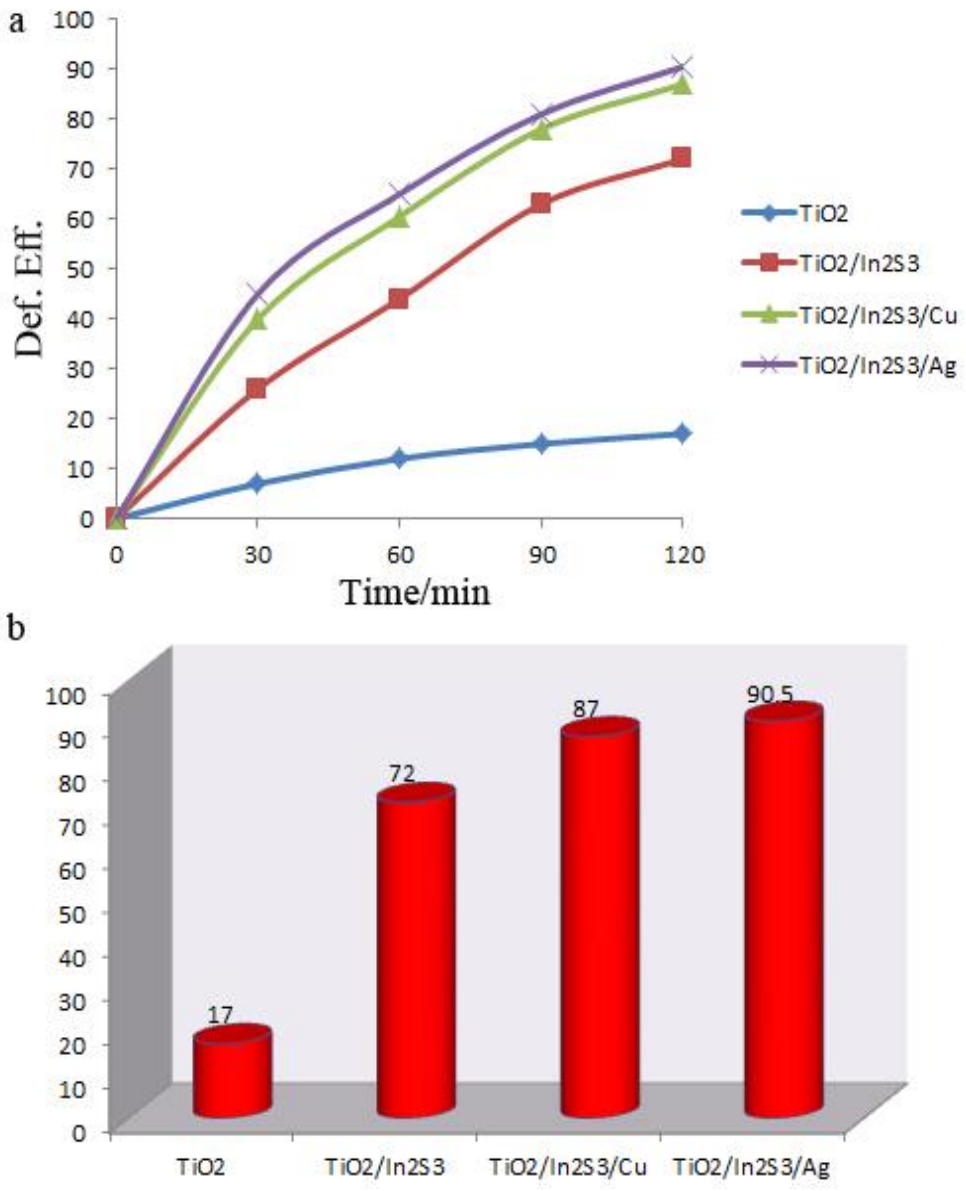

Fig. 8. Photocatalytic results for TiO_2, TiO_2/In_2S_3, TiO_2/In_2S_3/Ag composite, and TiO_2/In_2S_3/Cu nanocomposite.

Fig. 8 a and b illustrates the degradation results for RhB by TiO_2, TiO_2/In_2S_3, TiO_2/In_2S_3/Cu nanocomposites, and TiO_2/In_2S_3/Ag nanocomposites under visible light. Bare TiO_2 only degrades 17 % of RhB under 120 min of irradiation, while TiO_2/In_2S_3 degrades 72 of RhB during same irradiation time. This shows that In_2S_3 successfully boosted the photocatalytic activity of TiO_2 under visible light. By adding Cu and Ag to TiO_2/In_2S_3, degradation efficiency increased to 87 and 90 % from 72 %. Fig. 9 schematically describes how In_2S_3, Cu, and Ag boost degradation efficiency. As seen from Fig. 9, the electrons in the conduction band of In_2S_3 transferred to the conduction band of TiO_2. These electrons reacted with O_2 and generated active radicals that could degrade organic pollutions. On the other hand, holes in valance band of TiO_2 could jump to the valence band of In_2S_3 and reacted with H_2O and generate radical that could degrade organic

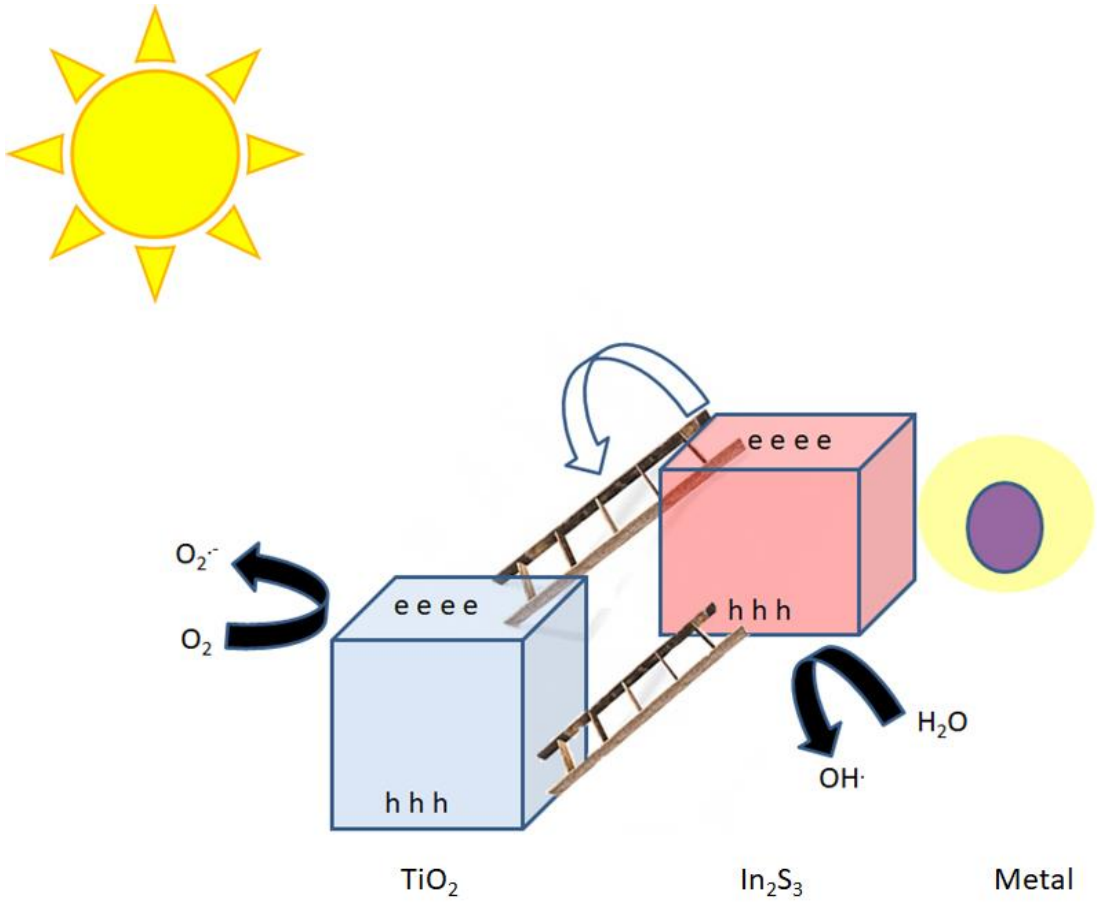

Fig. 9. Schematically describes how In_2S_3, Cu, and Ag boost degradation efficiency.

pollutions. Cu and Ag help to increased absorption and generated more electron and holes by their plasmonic effect.

CONCLUSION

In this research $TiO_2/In_2S_3/Cu$ nanocomposites and $TiO_2/In_2S_3/Ag$ nanocomposites were prepared by simple hydrothermal method. The aim was to extend the absorption peak of TiO_2 to the visible range and boost its photocatalytic activity under the visible light. Rhodamine B (RhB), Methyl orange (MO), Acid Black 1 (AB1), and Acid Brown 214 (AB214) as organic contaminations to study the photocatalytic activity of $TiO_2/In_2S_3/Cu$ nanocomposites and $TiO_2/In_2S_3/Ag$ nanocomposites were used to study the catalytic activity of $TiO_2/In_2S_3/Cu$ nanocomposites and $TiO_2/In_2S_3/Ag$ nanocomposites under the visible light. Results show $TiO_2/In_2S_3/Cu$ nanocomposites and $TiO_2/In_2S_3/Ag$ nanocomposites are highly efficient photocatalysts under visible light. Adding In_2S_3/Cu, and In_2S_3/Ag boosted the degradation efficiency to 87 and 90 % for RhB. $TiO_2/In_2S_3/Cu$ nanocomposites and $TiO_2/In_2S_3/Ag$ nanocomposites are characterized by using XRD, SEM, TEM, DRS, and EDX.

ACKNOWLEDGMENT

We would like to show our gratitude to the University of Raparin for supporting this work.

CONFLICT OF INTEREST

The authors declare that there is no conflict of interests regarding the publication of this manuscript.

REFERENCES

1. Lee K, Yoon H, Ahn C, Park J, Jeon S. Strategies to improve

the photocatalytic activity of TiO_2: 3D nanostructuring and heterostructuring with graphitic carbon nanomaterials. Nanoscale. 2019;11(15):7025-7040.
2. Schneider J, Matsuoka M, Takeuchi M, Zhang J, Horiuchi Y, Anpo M, et al. Understanding TiO_2 Photocatalysis: Mechanisms and Materials. Chem Rev. 2014;114(19):9919-9986.
3. Teymourinia H, Salavati-Niasari M, Amiri O, Yazdian F. Application of green synthesized TiO_2/Sb_2S_3/GQDs nanocomposite as high efficient antibacterial agent against E. coli and Staphylococcus aureus. Materials Science and Engineering: C. 2019;99:296-303.
4. Beshkar F, Amiri O, Salehi Z. Synthesis of $ZnSnO_3$ nanostructures by using novel gelling agents and their application in degradation of textile dye. Sep Purif Technol. 2017;184:66-71.
5. Saravanan R, Aviles J, Gracia F, Mosquera E, Gupta VK. Crystallinity and lowering band gap induced visible light photocatalytic activity of TiO_2/CS (Chitosan) nanocomposites. Int J Biol Macromol. 2018;109:1239-1245.
6. Cong Y, Zhang J, Chen F, Anpo M, He D. Preparation, Photocatalytic Activity, and Mechanism of Nano-TiO_2 Co-Doped with Nitrogen and Iron (III). The Journal of Physical Chemistry C. 2007;111(28):10618-10623.
7. Zhao D, Chen C, Wang Y, Ji H, Ma W, Zang L, et al. Surface Modification of TiO_2 by Phosphate: Effect on Photocatalytic Activity and Mechanism Implication. The Journal of Physical Chemistry C. 2008;112(15):5993-6001.
8. Luo Q, Ge R, Kang S-Z, Qin L, Li G, Li X. Fabrication mechanism and photocatalytic activity for a novel graphene oxide hybrid functionalized with tetrakis-(4-hydroxylphenyl) porphyrin and 1-pyrenesulfonic acid. Applied Surface Science. 2018;427:15-23.
9. Ouzzine M, Maciá-Agulló JA, Lillo-Ródenas MA, Quijada C, Linares-Solano A. Synthesis of high surface area TiO2 nanoparticles by mild acid treatment with HCl or HI for photocatalytic propene oxidation. Applied Catalysis B: Environmental. 2014;154-155:285-293.
10. Joost U, Šutka A, Oja M, Smits K, Döbelin N, Loot A, et al. Reversible Photodoping of TiO_2 Nanoparticles for Photochromic Applications. Chem Mater. 2018;30(24):8968-8974.
11. Liu J, Li Y, Ke J, Wang S, Wang L, Xiao H. Black NiO-TiO_2 nanorods for solar photocatalysis: Recognition of electronic structure and reaction mechanism. Applied Catalysis B: Environmental. 2018;224:705-714.
12. Xia X, Peng S, Bao Y, Wang Y, Lei B, Wang Z, et al. Control of interface between anatase TiO_2 nanoparticles and rutile TiO_2 nanorods for efficient photocatalytic H_2 generation. Journal of Power Sources. 2018;376:11-17.
13. Cheng J, Wang Y, Xing Y, Shahid M, Pan W. A stable and highly efficient visible-light photocatalyst of TiO_2 and heterogeneous carbon core–shell nanofibers. RSC Advances. 2017;7(25):15330-15336.
14. Reyes-Coronado D, Rodríguez-Gattorno G, Espinosa-Pesqueira ME, Cab C, de Coss R, Oskam G. Phase-pure TiO_2 nanoparticles: anatase, brookite and rutile. Nanotechnology. 2008;19(14):145605.
15. Islam S, Nagpure S, Kim D, Rankin S. Synthesis and Catalytic Applications of Non-Metal Doped Mesoporous Titania. Inorganics. 2017;5(1):15.
16. Choi J, Park H, Hoffmann MR. Effects of Single Metal-Ion Doping on the Visible-Light Photoreactivity of TiO_2. The Journal of Physical Chemistry C. 2009;114(2):783-792.
17. Dunnill CW, Parkin IP. Nitrogen-doped TiO_2 thin films: photocatalytic applications for healthcare environments. Dalton Trans. 2011;40(8):1635-1640.
18. Zhang H, Zhang Y, Yin J, Li Z, Zhu Q, Xing Z. In-situ N-doped mesoporous black TiO_2 with enhanced visible-light-driven photocatalytic performance. Chemical Physics. 2018;513:86-93.
19. Lindgren T, Mwabora JM, Avendaño E, Jonsson J, Hoel A, Granqvist C-G, et al. Photoelectrochemical and Optical Properties of Nitrogen Doped Titanium Dioxide Films Prepared by Reactive DC Magnetron Sputtering. The Journal of Physical Chemistry B. 2003;107(24):5709-5716.
20. Amiri O, Salavati-Niasari M, Bagheri S, Yousefi AT. Enhanced DSSCs efficiency via Cooperate co-absorbance (CdS QDs) and plasmonic core-shell nanoparticle (Ag@PVP). Sci Rep. 2016;6(1).
21. Song Y, Li N, Chen D, Xu Q, Li H, He J, et al. N-Doped and CdSe-Sensitized 3D-Ordered TiO_2 Inverse Opal Films for Synergistically Enhanced Photocatalytic Performance. ACS Sustainable Chemistry & Engineering. 2018;6(3):4000-4007.
22. Sabet M, Salavati-Niasari M, Amiri O. Using different chemical methods for deposition of CdS on TiO_2 surface and investigation of their influences on the dye-sensitized solar cell performance. Electrochimica Acta. 2014;117:504-520.
23. Amiri O, Salavati-Niasari M, Rafiei A, Farangi M. 147% improved efficiency of dye synthesized solar cells by using CdS QDs, Au nanorods and Au nanoparticles. RSC Adv. 2014;4(107):62356-62361.
24. Ma K, Yehezkeli O, Domaille DW, Funke HH, Cha JN. Enhanced Hydrogen Production from DNA-Assembled Z-Scheme TiO_2 –CdS Photocatalyst Systems. Angew Chem Int Ed. 2015;54(39):11490-11494.
25. Chandra M, Bhunia K, Pradhan D. Controlled Synthesis of CuS/ TiO_2 Heterostructured Nanocomposites for Enhanced Photocatalytic Hydrogen Generation through Water Splitting. Inorganic Chemistry. 2018;57(8):4524-4533.
26. Singh Sekhon J, S Verma S. Refractive Index Sensitivity Analysis of Ag, Au, and Cu Nanoparticles. Plasmonics. 2011;6(2):311-317.
27. M KK, K B, G N, B S, A V. Plasmonic resonance nature of Ag-Cu/ TiO_2 photocatalyst under solar and artificial light: Synthesis, characterization and evaluation of H 2 O splitting activity. Applied Catalysis B: Environmental. 2016;199:282-291.